BUILDINGS & CITIES

Assessing the influence of neighbourhood-scale vertical greening application

RESEARCH

KANCHANE GUNAWARDENA
KOEN STEEMERS
*Author affiliations can be found in the back matter of this article

ubiquity press

ABSTRACT

The warming climate is expected to increase environmental thermal loading on urban buildings. Green infrastructure enhancements have been widely supported as a means to address the resulting heat-related risks, with the challenge of realising enhancements in densely built cities necessitating the consideration of vegetated architectural features. Early efforts promoted horizontal greening, although in recent years 'vertical greening' has gained increased prominence. This paper examines the hypothesis that the wider implementation of the latter typology could serve to enhance urban climate resilience, and does so by applying an analysis pathway including the coupling of a novel one-dimensional vertical greening model (VGM) with an urban climate simulation framework to estimate the microclimate and energy-use implications of neighbourhood-scale vertical greening. The simulation results highlighted immediate thermal relief to canyon pedestrians, as well as net annual space-conditioning energy savings for the canyon buildings. These benefits, however, were modest, with a relatively pronounced influence offered for the urban neighbourhood than suburban, and with the living wall category than green facade application. Although the annual savings present potential for the wider implementation in temperate climates, the influence is insufficient to offer it as an exclusive solution, with any widescale application also requiring assessment against other ecosystem benefits and maintenance costs.

PRACTICE RELEVANCE

The study contributes to the evidence base supporting both policy and practice targeting the delivery of green infrastructure enhancements, by presenting evidence that addresses widescale evergreen vertical greening application potential in temperate climates. It emphasises the need for key decision-makers considering such strategies to acknowledge the magnitude of thermal and energy-use benefits that can be reasonably expected, and

CORRESPONDING AUTHOR:

Kanchane Gunawardena

The Martin Centre for Architectural and Urban Studies, Department of Architecture, University of Cambridge, 1–5 Scroope Terrace, Cambridge CB2 1PX, UK

krag2@cantab.ac.uk

KEYWORDS:

energy use; green facades; green infrastructure; living walls; microclimates; space conditioning; street canyon; urban climate; urban heat island; urban morphology; vertical greening

TO CITE THIS ARTICLE:

Gunawardena, K., & Steemers, K. (2023). Assessing the influence of neighbourhood-scale vertical greening application. *Buildings and Cities*, 4(1), pp. 103–123. DOI: https://doi.org/10.5334/bc.282

identifies the most appropriate application typology and siting to prioritise. Finally, the study demonstrates the application of a novel VGM-coupled analysis pathway, which allows for such considerations to be frontloaded to building and urban design approaches. This in turn will offer technically sound reasoning when specifying such strategies and prevent costly failures of future installations.

1. INTRODUCTION

To address worsening heat-related risks in cities, green infrastructure enhancements have been widely supported in recent years. The challenge of realising such enhancements in densely built cities has necessitated the consideration of spatially efficient alternatives that are described collectively as 'vegetated architectural features' (Gunawardena *et al.* 2017c; Gunawardena & Kershaw 2016). Early initiatives promoted horizontal greening solutions (*i.e.* green roofing), although in recent years 'vertical greening' (VG) has gained increased attention as means to exploit the underused and abundant vertical surfaces of urban buildings. Such installations are thus becoming commonplace in many cities, while their technical assessment to determine thermal interactions and resultant energy saving potential is an emerging area of research interest (Gunawardena & Steemers 2019b).

The available studies of such systems, including the principal categories of green facades (GF) (when climbing plants are grown along a wall) and living walls (LW) (when many plant types are planted into a vertically supported substrate zone), have highlighted significant surface and proximate air temperature cooling (Wong *et al.* 2010). The limited wintertime studies available have also highlighted GF to provide beneficial warming (Bolton *et al.* 2014; Cameron *et al.* 2015), while LW in certain circumstances could present the converse (Tudiwer & Korjenic 2017). With both categories, these influences seem to be pronounced on the harshest of summer and winter days (de Jesus *et al.* 2017), with cooling during the daytime and potential warming during the night-time expected (Koyama *et al.* 2013). These thermal enhancements in return have been suggested to offer summer cooling and winter heating energy-use benefits to buildings, although the limited body of evidence is at present biased towards emphasising summertime benefits (Gunawardena & Steemers 2019b).

This paper is concerned with the hypothesis that the wider implementation of VG, including GF and LW, could serve to enhance climate resilience in urban built environments. It examines this by considering neighbourhood-scale street canyon applications, with a comparison study between office building construction build-ups including such installations sited within the morphological contexts of central urban and suburban neighbourhoods. This is achieved through the simulation of the respective street canyons, using a multiscale urban climate framework including the coupling of a novel vertical greening model (VGM) introduced by Gunawardena (2021).

1.1 SIMULATING VERTICAL GREENING INFLUENCE IN URBAN CLIMATES

The best means of accounting for urban site-specific climate loading is by sourcing measurement data from direct methods to compile a localised weather profile. For such measurements to be representative, long-term data collection is necessary to address the dynamic variance of an urban heat island's (UHI) influence (Oke 1987). This prerequisite favours the use of high-resolution networks of fixed stations, as opposed to mobile traverse data collection. There is, however, no accepted standard practice currently in place to direct such fixed-station measurement campaigns (Grimmond *et al.* 2010). This means that new studies would have to establish their own networks at the representative grid resolution required. Although such measurement projects exist (*e.g.* Kolokotroni *et al.* 2007), the infrastructural cost to achieve similar data collection campaigns is unlikely to be available for typical urban site assessments (Gunawardena 2018a).

In order to approximate urban climate influence on specific sites, this study instead considered the model framework published as the 'Urban Weather Generator' (UWG) V4.1.0 (Bueno *et al.* 2013, 2015), and used its modified version, V5.2.0 beta (Bueno *et al.* 2019). This framework is based on

multiscale energy balances and Monin-Obukhov similarity theory (Monin & Obukhov 1988), and is composed of the following four coupled sub-models: rural station model (RSM), vertical diffusion model (VDM), urban boundary-layer model (UBLM) and urban canopy and building energy model (UC-BEM). A summary of the principal data interactions of this framework is shown in Figure 1, while detailed mathematical descriptions are given by Bueno *et al.* (2013, 2014), and field data validations and applications by Bueno *et al.* (2013, 2014) and Nakano *et al.* (2015). The principal modifications included in UWG V5.2.0 beta (Bueno *et al.* 2019) are described by Gunawardena *et al.* (2019) and Gunawardena (2021), with corresponding framework application studies presented by Gunawardena (2018a, 2018b), Gunawardena & Kershaw (2017) and Gunawardena & Steemers (2019a). The framework is primed with the input of a rural weather file, which is used by the sub-models to calculate the principal outcomes of canyon-specific air temperature (T_{can}) and relative humidity (RH_{can}). The output is compiled as a modified canyon weather file in the EnergyPlus (*epw*) format, which can then be used by any dynamic building thermal modelling software (Gunawardena 2018b).

The earliest VG modelling exercises adapted existing vegetation canopy models to consider idealised scenarios. These typically used empirical priming data, as exemplified by the approaches of Di & Wang (1999) and Holm (1989). An alternative approach considered priming using a reference plant community. The latent flux in such models is calculated for a reference water stress-free horizontal plant canopy, using the United Nations' Food and Agriculture Organization's (FAO) adaptation of the Penman–Monteith model (Allen *et al.* 1998) and then multiplied by a factor that accounts for species-specific vegetation characteristics such as canopy height, roughness and stomatal responses to environmental loading. The resulting application studies have predominantly used published FAO crop factors either directly or as a close approximation to what it would be for the vegetation community assessed (Davis *et al.* 2019). This reliance on empirically derived crop factors relating to horizontal canopies means that the method is best suited for considering monoculture systems with uniform coverage. This is a challenging limitation for considering GF given their inconsistent coverage, as well as for LW given the canopy diversity of typically implemented plant communities. The most common modelling approach taken to date has considered the adaptation of existing horizontal greening (green roof) models, given their development preceded interest in VG. Dynamic models developed by Alexandri & Jones (2007) and Sailor (2008), for example, were integrated as a module in the building energy model EnergyPlus, followed by several application studies (Olivieri *et al.* 2017). Djedjig *et al.* (2012, 2016) similarly adapted their green-roof model to present a series of studies where they coupled it with a mass flow model and the building energy model TRNSYS. The principal issue with these adaptation approaches is that they are not readily adaptable to examine different system configurations. To address this, researchers have pursued the development of a VGM from first principles. A notable example is the model by Susorova *et al.* (2013) that simulates the one-dimensional horizontal heat flux through a vertical plant layer. The principal limitation of this simplified model is that it only provides an opportunity to consider direct GF.

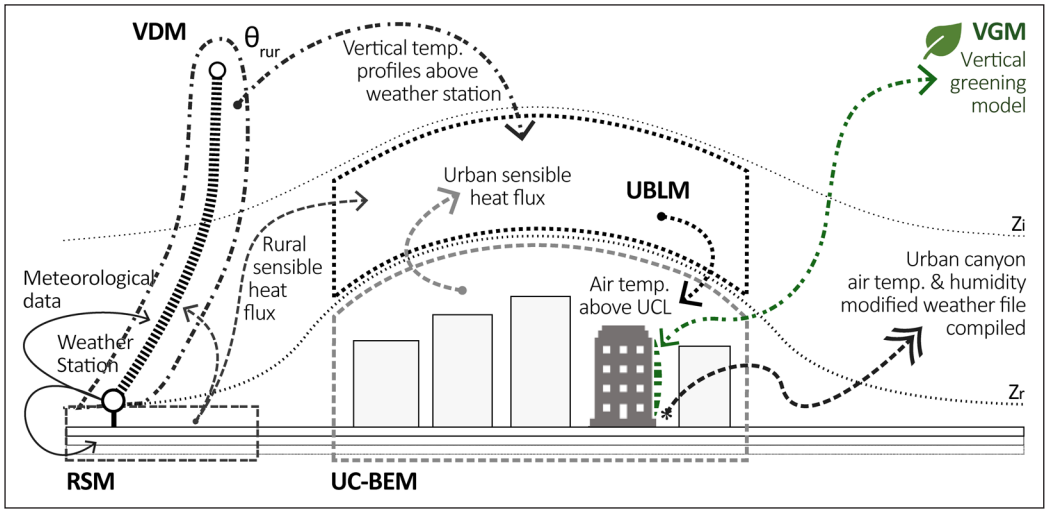

Figure 1: Modified urban framework pathway, including the vertical greening model (VGM) coupling.

To simulate VG applications on urban street canyon building walls, this study used the novel one-dimensional VGM developed and validated by Gunawardena (2021) and coupled it with the aforementioned UWG framework (Figure 1). The inclusion of a VG system is considered in this VGM as the addition of a 'layer(s)' to the face of a new or existing host-wall construction. For direct GF this takes the form of a 'plant layer' with a certain leaf area index (LAI), while for LW a saturated 'substrate layer' is also included between the plant layer and host structure (Gunawardena & Steemers 2022). The model's code was first modified to be compatible with the data (input/output) exchanges of the UWG framework and then coupled via its 'element class', which calculates building envelope surface flux and passes these to its UC-BEM to calculate the canyon surface flux. This coupled approach presents a computationally efficient analysis pathway able to complete full annual simulations with hourly resolution outputs (Gunawardena 2021).

1.2 ASSESSING CASE STUDIES IN LONDON'S HEAT ISLAND

The unique climate of cities is explained by the UHI effect, the warming experienced relative to their surroundings (Oke 1987). The earliest recorded heat island observations are of London (temperate/Cfb Köppen climate), when in 1833 Luke Howard identified it to be 0.6 K warmer in the summer and 1.2 K warmer in the winter than its surroundings. He also observed it to be warmest at night by 2.05 K, while during the day it was 0.18 K cooler to demonstrate a modest 'cool island' effect (Howard 1833). London's relative warming has since been studied by many longitudinal surveys, notably Moffitt (1972) identified an about 0.8 K warming (between 1878 and 1968), and Chandler (1965) identified 1.4 K warming (between 1931 and 1960), with 1.6 K summer and 1.2 K winter monthly means. More recent time-series analyses have found the increasing warming trend observed in the preceding century to have waned (Jones & Lister 2009; Lee 1992). Considering these observations, Central London sites are projected to maintain their heat island intensity (ΔT_{UHI}), while sites in suburban areas are likely to demonstrate intensification (Jones & Lister 2009). A significant variable determining the experience of this trend is therefore the radial distance from the city's thermal core (Kolokotroni *et al.* 2009; Wilby 2003). Watkins *et al.* (2002) found 77% of the measured night-time temperature variance to be strongly correlated with this distance, with the thermal core identified as the City of London. These observations suggested the transition in morphologies and materiality typically observed when traversing from the city core to the peripheries to be significant variables affecting the potency of the heat island load experienced at specific sites, with future densification trends likely to influence intensification.

London's heat island maxima and minima are assessed mostly by higher resolution studies, typically targeting central sites, monitored for limited durations. As summertime examples, Watkins *et al.* (2002) had recorded peaks of about 7 K, Kolokotroni & Giridharan (2008) had recorded day- and night-time peaks of about 9 K, while Doick *et al.* (2014) had recorded higher nocturnal peaks of about 10 K. Wintertime studies have also highlighted high peaks, with Giridharan & Kolokotroni (2009) notably having recorded day- and night-time peaks of about 9 K. In summary, these examples present ample evidence for ΔT_{UHI} maxima reaching high values at central sites during the day- and night-time and throughout the year. However, a comparison between urban core values and those at the peripheries is difficult to consider, given that studies seldom attempt to assess the intermediary condition represented by suburban neighbourhoods.

To assess VG influence in urban environments, this study considered the urban core with a selected site where heat island intensity is expected to be at its highest, as well as a suburban site where it is expected to be less potent. These case study morphologies are respectively defined here as the Moorgate and Wimbledon neighbourhoods of London (Figure 2). Moorgate is located within the City of London, the city's thermal core (radial origin) as identified by Watkins *et al.* (2002). It is regarded as the financial centre and typically includes many banks housed in Portland stone-faced traditional buildings. Wimbledon, in contrast, represents the suburban

condition located in south-west London (about 15 km from the thermal core/radial origin), typically represented by residential and retail buildings with dominant brick-faced facades. Although there are expansive green spaces in Wimbledon (*i.e.* Wimbledon Common), the area selected for the study represents a built-up area to the south, and thus is upwind of dominant south-westerly flow experienced in London (green-space influence is greater downwind) (Gunawardena *et al.* 2017c). It is presently characterised as a residential neighbourhood of moderate density.

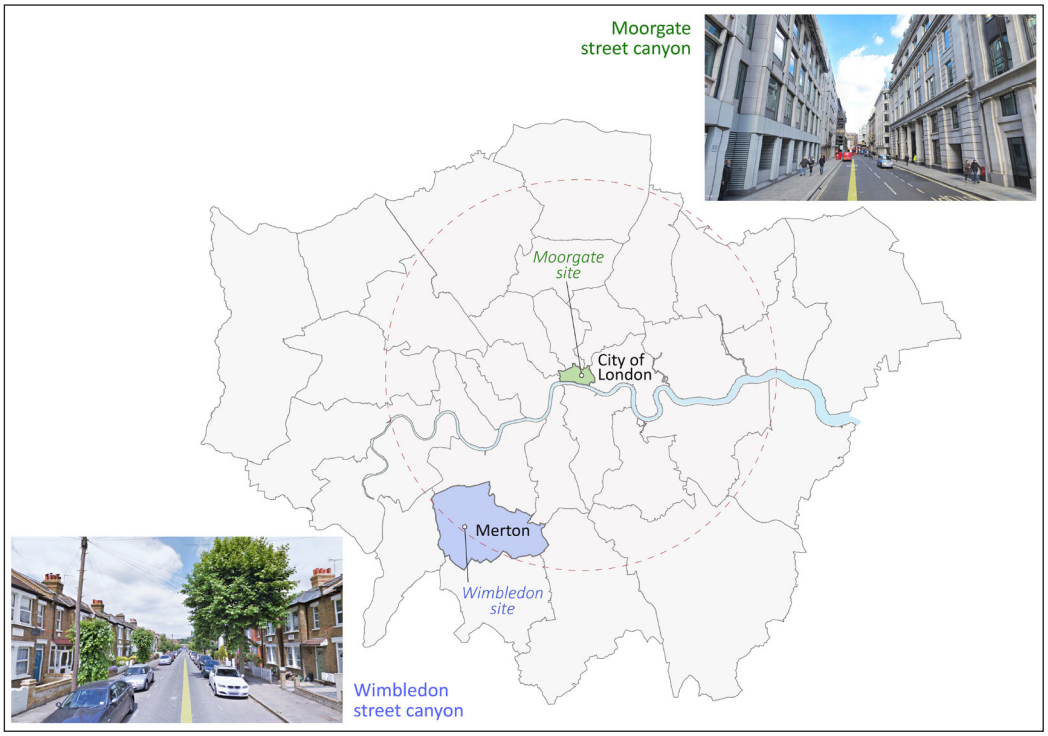

Figure 2: Case study locations of 'central urban' Moorgate and 'suburban' Wimbledon in London, and typical north- to south-oriented street canyon views.

Source: Google Earth, Street-view, 2019.

2. METHODOLOGY

2.1 DEFINING CASE STUDIES

The case study urban morphologies of both Moorgate and Wimbledon were idealised by averaging parameters to generate roughness profiles with a 500 m characteristic radius. At both near north- to south-oriented street canyons, the buildings on either side were given the same use, occupancy schedule, and space-conditioning (heating and cooling) and gains profiles of a medium-sized office building, and only differed between scenarios described in Table 1, in terms of their facade constructions detailed in Tables 2 and 3. These roughness and material profiles (including evergreen vegetation data, where applicable), together with a rural weather file were then input to the UWG (V5.2.0 beta) + VGM coupling, to generate new canyon climate and energy consumption data for the respective scenarios.

The rural weather dataset used for this study is from the design summer year (DSY) for the Reading area, created using the UKCP09 Weather Generator (described by Eames *et al.* 2011). This input weather data represent the rural boundary condition where the influence of the city of London is assumed to be negligible. The Reading file was selected for this purpose as it represents conditions well beyond urbanised London, while preceding research has confirmed the heat island of the city itself to make negligible contribution to the gridded data output of the UKCP09 Weather Generator (Kershaw *et al.* 2010). The weather file also presented clear conditions for both the summer and winter solstices (low cloud cover), which represents ideal conditions for heat island formation and serve as benchmark days to compare and assess the different canyon climates generated (Gunawardena & Steemers 2019a).

SCENARIO	WEATHER DATA USED	CONSTRUCTIONS (DETAILED IN *TABLE 2*)
Urban/'*Urb*' (Moorgate)		
Urb-Stone (*base*)	Reading DSY modified using the UWG to include heat island influence	*Base scenario:* Using stone facades with a glazing ratio (GR) = 0.30
Urb-GF	Reading DSY modified using the UWG to include heat island influence and canyon GF cover	*GF scenario:* Using stone facades with a direct GF and GR = 0.30
Urb-LW	Reading DSY modified using the UWG to include heat island influence and canyon LW cover	*LW scenario:* Using stone facades with a LW and GR = 0.30
Suburban/'*SUrb*' (Wimbledon)		
SUrb-Brick (base)	Reading DSY modified using the UWG to include heat island influence	*Base scenario:* Using brick facades with GR = 0.30
SUrb-GF	Reading DSY modified using the UWG to include heat island influence and canyon GF cover	*GF scenario:* Using brick facades with a direct GF and GR = 0.30
SUrb-LW	Reading DSY modified using the UWG to include heat island influence and canyon LW cover	*LW scenario:* Using brick facades with a LW and GR = 0.30

Table 1: Simulation scenarios considered.

Note: GF = green facade; DSY = design summer year; LW = living wall; UWG = Urban Weather Generator.

PARAMETER		MOORGATE (CENTRAL URBAN)	WIMBLEDON (SUBURBAN)
Urban/suburban building block	Canyon block dimensions (L × D × H)	60 × 35 × 24.5 m	60 × 35 × 24.5 m
	Context block dimensions (L × D × H)	60 × 35 × 24.5 m	60 × 35 × 10.5 m
	Mean floor height	3.5 m	
	Assumed building use	Medium office	
Simplified base building constructions (existing)	Wall type	Stone	Brick
	Materials	Portland stone/plaster	Brick/gypsum plaster
	Thickness	0.3/0.025 m	0.215/0.035 m
	U-value	2.33 $W \cdot m^{-2} \cdot K^{-1}$	1.96 $W \cdot m^{-2} \cdot K^{-1}$
	Surface material albedo	0.62	0.30
	Emissivity	0.90	0.93
	Thermal conductivity	1.70 $W \cdot m^{-1} \cdot K^{-1}$	0.84 $W \cdot m^{-1} \cdot K^{-1}$
	Specific heat capacity	1,000 $J \cdot kg^{-1} \cdot K^{-1}$	800 $J \cdot kg^{-1} \cdot K^{-1}$
	Thermal diffusivity	0.77 $mm^2 \cdot s^{-1}$	0.62 $mm^2 \cdot s^{-1}$
	Glazing ratio	0.3 (30%)	
	U-value	1.93 $W \cdot m^{-2} \cdot K^{-1}$	
	Roof type	Flat	Inclined (45°)
	Materials:	Gravel/expanded polystyrene/concrete/ceiling tiles	Clay tiled/timber insulation/gypsum plasterboard
	Thickness	0.075/0.1/0.3/0.05 m	0.015/0.1/0.25/0.015 m
	U-value	0.24 $W \cdot m^{-2} \cdot K^{-1}$	0.23 $W \cdot m^{-2} \cdot K^{-1}$
Priming	Initial construction temperature	20°C	
Building gains	Lighting and equipment	12 and 25 $W \cdot m^{-2}$	
	Occupancy	6 m^2 per person	
	Gains profile used	Weekdays: 07:00–19:00 hours with a 0.9 load Saturday: 07:00–17:00 hours with a 0.4 load Sunday: full day with a 0.1 load	

(Contd.)

PARAMETER		MOORGATE (CENTRAL URBAN)	WIMBLEDON (SUBURBAN)
Building space-conditioning	Infiltration	0.5 ach	
	Ventilation	0.002 $m^3 \cdot s^{-1} \cdot m^{-2}$	
	Cooling system	Air	
	Heating efficiency	0.80	
	Heating setpoint schedule	Weekdays and Saturday: 00:00–05:00 hours at 5°C; 05:00–06:00 hours at 15°C; 06:00–22:00 hours at 20°C; 22:00–23:00 hours at 15°C; and 23:00–00:00 hours at 5°C Sundays: full day at 5°C	
	Cooling setpoint schedule	Weekdays: 00:00–05:00 hours at 35°C; 05:00–06:00 hours at 27°C; 06:00–22:00 hours at 23°C; 22:00–23:00 hours at 27°C; and 23:00–00:00 hours at 35°C Saturday: 00:00–06:00 hours at 35°C; 06:00–18:00 hours at 23°C; 18:00–19:00 hours at 27°C; and 19:00–00:00 hours at 35°C Sunday: 00:00–06:00 hours at 35°C; 06:00–18:00 hours at 50°C; and 18:00–00:00 hours at 35°C	
	Heat rejected to canyon	50%	25%[b]
Roads	Material and thickness	Asphalt/0.5 m	
Urban/suburban	Vegetation coverage ratio	Urban: 0.005 Rural: 0.8	0.2 0.8
Neighbourhood urban/suburban	Mean building height[a]	24.5 m	10.8 m
	Horizontal building density ratio[a]	0.598	0.480
	Vertical to horizontal area ratio[a]	0.99	0.35
	Tree coverage ratio	0.001	0.080
	Non-building sensible heat rejection	22.68 $W \cdot m^{-2}$	1.77 $W \cdot m^{-2}$
	Non-building latent heat rejection	2.268 $W \cdot m^{-2}$	0.18 $W \cdot m^{-2}$
	Daytime boundary-layer height	1,000 m	850 m
	Night-time boundary-layer height	80 m	50 m
	Characteristic neighbourhood length	500 m	
	Tree and grass latent fractions	0.7 and 0.5	
	Contextual Vegetation albedo	0.25	
	Contextual Vegetation contribution, start to end	April–September (deciduous)	
Reference weather site	Latitude, longitude (for Reading)	51.446, –0.957	
	Distance from the study sites	~60 km due west	~52 km due west

PARAMETER		GREEN FACADE (GF)	LIVING WALL (LW)
VG construction (hypothetical)	Materials	Evergreen climbing plants (*Hedera helix*)/host wall	Herbaceous evergreens/saturated soil (substrate)/host wall
	Canopy depth	Canopy depth 0.2 m, and rest of the build-up as per ***Table 2***	0.25/0.1 m, and rest as per **Table 2**
	U-value (excluding host wall)	1.49 $W \cdot m^{-2} \cdot K^{-1}$	0.46 $W \cdot m^{-2} \cdot K^{-1}$
	Wall vegetation coverage ratio	0.5 (50%)	
Vegetation (evergreen)	Canopy absorptivity	(1–albedo–transmissivity)	
	Canopy albedo	0.20	
	Canopy emissivity	0.95	

(Contd.)

Table 2: Parameter inputs used for simulations.

Note: [a] Essential neighbourhood morphological parameters.

[b] Building heat rejection to the suburban canyon is lower owing to the reduced contextual building heights and resultant greater coupling with the bulk atmosphere (Gunawardena *et al.* 2019).

PARAMETER		GREEN FACADE (GF)	LIVING WALL (LW)
	Leaf width	0.075 m	0.060 m
	Open stomatal conductance	0.30 $mol \cdot m^{-2} \cdot s^{-1}$	0.20 $mol \cdot m^{-2} \cdot s^{-1}$
	Closed stomatal conductance	0.01 $mol \cdot m^{-2} \cdot s^{-1}$	
	Radiation attenuation coefficient	0.5 (assumed)	
	Stomatal arrangement	Hypostomatous	Amphistomatous (assumed)
	Leaf angle	45° (assumed)	
Substrate (LW only)	Density	n.a.	1,230 $kg \cdot m^{-3}$
	Specific heat capacity	n.a.	1,140 $J \cdot kg^{-1} \cdot K^{-1}$
	Volumetric heat capacity	n.a.	2,310,000 $J \cdot m^{-3} \cdot K^{-1}$
	Surface albedo	n.a.	0.4
	Surface emissivity	n.a.	0.9
	Permanent wilting soil moisture threshold (η_{wilt})	n.a.	0.39 (peat soil)
	Root zone min. soil moisture (η_{root})	n.a.	0.70 (assumed)

Table 3: Construction parameters of vertical greening (VG) additions.

2.2 LIMITATIONS OF THE SIMULATION PATHWAY

It is significant to note here key limitations of the coupled analysis pathway to best interpret the simulation results presented below. Beyond the established limitations of the UWG framework, VGM validation results had highlighted relatively weaker agreement during warm summer daytime conditions. This was attributed to surface air movement, observed at monitored studies (Gunawardena & Steemers 2020, 2021). Air movement off the installation surface translates to modifications in both lateral and vertical heat flux, as well as mass flow (vertical influences are of greater significance). The VGM's limitation of only considering one-dimensional horizontal heat flux excludes such lateral and vertical modifications in the energy balance (Gunawardena 2021). This means that best approximations are for limited vertical canopy layer spans, and thus it is inappropriate for assessing irregular morphologies with tall buildings. This limitation complements the same requirement of the UWG's application and was considered when selecting the case studies (*i.e.* canyons belonging to uniform morphological contexts).

It is also worth noting that for most plant parameters the VGM makes several assumptions to reduce user-specified input burden and maintain computational efficiency. Plant thermal resistance, leaf width, leaf area index, canopy attenuation coefficient, leaf absorptivity and stomatal conductance are thus treated as a constant for the active season defined, while leaf angle, canopy distribution and orientation are assumed to be static. Air proximate to stomatal pores is also assumed to be unsaturated, and substrate moisture at roots is defined as a constant (*i.e.* no water stress and constant water use rate), while diffusion variance and precipitation contributions are also not currently included (Gunawardena 2021).

3. FINDINGS

Results from pathway applications were first used to characterise the respective canyon climates generated (for the scenarios in Table 1). The output was then used to characterise exterior building wall temperatures ($T_{canWall}$) and resulting surface flux modifications, followed by indoor space-conditioning energy consumption impact for the buildings facing the respective canyons (normalised and reported as consumption per m^2 of building area).

3.1 CANYON MICROCLIMATE PROFILES

From the simulated heat island data, daily maximum and minimum intensity (ΔT_{UHI}) values present an understanding of the expected extremes (Figure 3a). The highest summertime mean for daily maxima was presented by the urban GF scenario (*Urb-GF* = 4.41, ±2.32 K, *N* = 153 summer days), while the lowest was presented by the suburban base brick scenario (*SUrb-Brick* 3.29, ±2.09 K). The highest summertime mean for the daily minima was presented by the urban base stone scenario (*Urb-Stone* = 0.20, ±0.54 K), while the lowest was presented by the suburban LW scenario (*SUrb-LW* = –0.32, ±0.52 K). Notably the mean daily minima for all urban scenarios presented positive values, while all suburban scenarios presented negative values to suggest greater 'cool island' conditions. These daily minima means, however, do not capture the frequency of cool island occurrences simulated owing to the contribution from positive minima. For this reason, hourly resolution data must be examined.

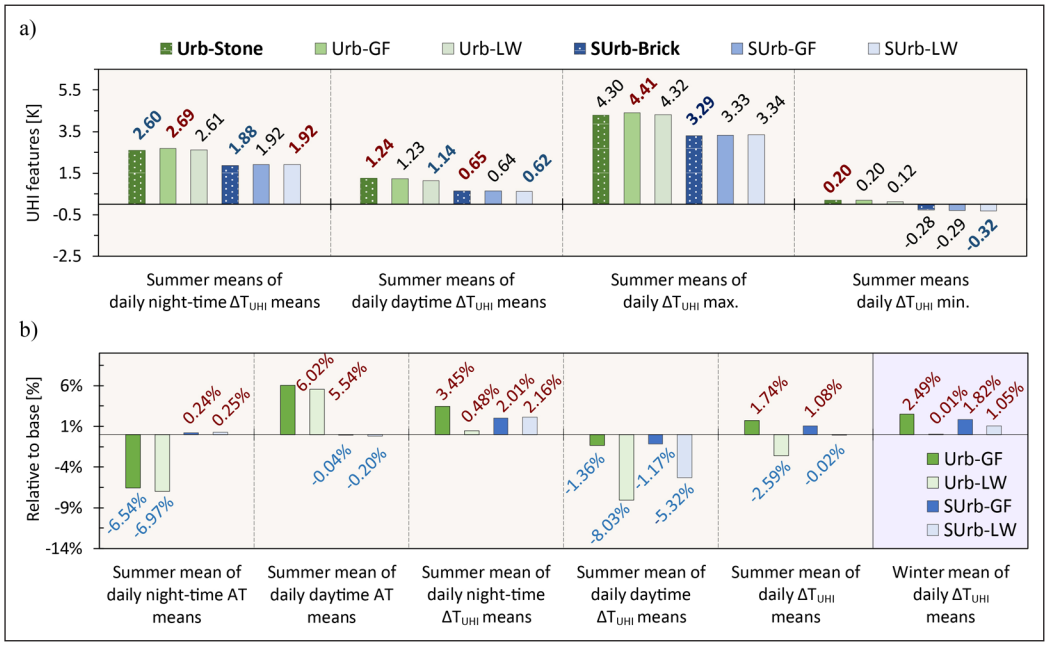

Figure 3: (a) Summertime means of daily heat island intensity (ΔT_{UHI}) features; and **(b)** modifications of summertime means following vertical greening applications, air temperature (AT) and heat island intensity features.

When the hourly resolution of heat island intensities were examined, cool island occurrences were identified in all scenarios with intensities ranging between < 0 and –2.5 K. The highest urban occurrences were presented by the LW scenario (*Urb-LW* = 4.0%, *N* = 3672 hours), in contrast to the lowest presented by the base stone scenario (*Urb-Stone* = 2.9%). Notably the suburban scenarios showed a significantly higher representation, with the highest presented by the LW scenario (*SUrb-LW* = 9.2%), and lowest by the base brick scenario (*SUrb-Brick* = 8.2%). The hourly resolution data also identified significant peak values ranging between > 6.5 and ≤ 12.5 K. The highest urban occurrences were presented by the GF scenario (*Urb-GF* = 3.0%, *N* = 3672), in contrast to the lowest presented by the LW scenario (*Urb-LW* = 2.7%). Notably, the suburban scenarios presented a much lower representation, all around 1% of the total summertime hours simulated.

When all hours of the day were included (*i.e.* 24 h), urban summertime ΔT_{UHI} means were considerably higher than for suburban scenarios (0.65, 0.67 and 0.60 K warmer relative to suburban base brick, GF and LW scenarios, respectively). When the hours of the day were divided between daytime (12 h from 06:00 to 18:00) and night-time (the residual hours) ΔT_{UHI} (Figure 3a), the highest night-time urban mean was presented by the LW scenario (*Urb-LW* = 2.69, ±1.38 K), while the lowest was presented by the base stone scenario (*Urb-Stone* = 2.60, ±1.37 K). With the suburban means, the highest was again presented by the LW scenario (*SUrb-LW* = 1.92, ±1.13 K), while the lowest was presented by the corresponding base brick scenario (*SUrb-Brick* = 1.88, ±1.11 K). Considering the lower daytime means, the highest urban mean was presented by

the base stone scenario (*Urb-Stone* = 1.24, ±0.59 K), while the lowest was presented by the LW scenario (*Urb-LW* = 2.60, ±1.37 K). With the suburban daytime means, the highest was presented by the corresponding base brick scenario (*SUrb-Brick* = 0.65, ±0.47 K), while the lowest was again presented by the LW scenario (*SUrb-LW* = 0.62, ±0.47 K). Across all scenarios night-time ΔT_{UHI} means were consistently higher than daytime, with VG applications having served to increase nocturnal means, while daytime means in contrast were reduced (Figure 3b).

When the summertime day/night divide of hourly ΔT_{UHI} maxima and minima were considered, the urban context generated greater night-time maxima occurrences (where ΔT_{UHI} was > 6.5 K; *Urb-Stone* = 4.18%, relative to *SUrb-Brick* = 1.37%). The application of VG modified these summertime hourly occurrences for the urban setting from 4.18% to 4.64% and 4.12% with the GF and LW applications, respectively. For the suburban setting the GF application affected no change to maintain occurrences at 1.37%, while the LW application marginally increased it to 1.44%. The LW application therefore reduced night-time hourly ΔT_{UHI} maxima occurrences in the urban setting, by 1.6% in the summer and annually by 2.8%, relative to the base stone or *Urb-Stone* scenario. With summer daytime cool island conditions, the suburban context presented greater hourly occurrences (*SUrb-Brick* = 19.48%, relative to *Urb-Stone* = 6.73%). VG applications increased these cool island occurrences for the urban setting from 6.73% to 7.52% and 9.35% for the GF and LW applications, respectively, while for the suburban setting, these occurrences were also increased from 19.48% to 20.07% and 20.13%, respectively.

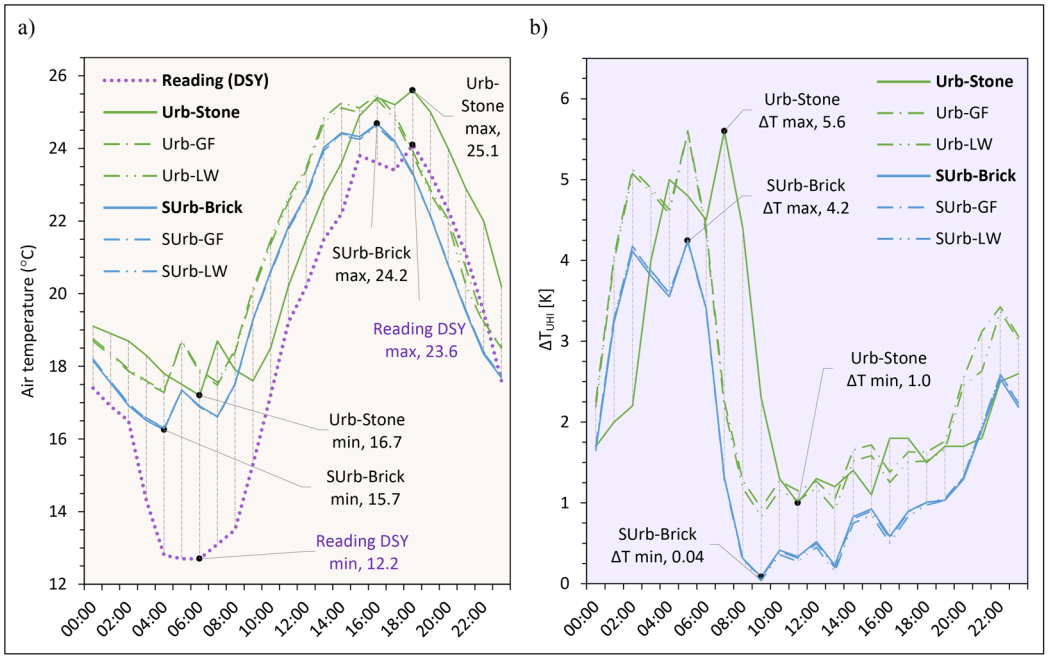

Figure 4: (a) Summer solstice T_{can} profiles relative to the Reading design summer year (DSY) profile; and **(b)** summer solstice ΔT_{UHI} (intensity) profiles for the scenarios simulated.

While the above observations can be made for mean values, examining daily profiles highlighted distinct features. For example, profiles for the summer solstice (21 June) highlighted the situation when the ΔT_{UHI} maximum for the day was reached after sunrise (around 04:50), at around 05:30 for the *SUrb-Brick*, and much later and with greater intensity at around 07:30 for the *Urb-Stone* scenario (Figure 4). Notably, the addition of VG (GF or LW) to the *Urb-Stone* base scenario meant that this peak was reached much earlier (*i.e.* nearly nullified the lag), to be around the same time as all *SUrb-Brick* scenarios. The summer solstice profiles also showed greater variation between urban GF and LW profiles relative to the *Urb-Stone* base scenario, while the suburban profiles were broadly similar for all. In general, the daily profiles highlighted urban setting ΔT_{UHI} profiles to be much higher in amplitude (*i.e.* warmer), than corresponding suburban profiles (Figure 4b).

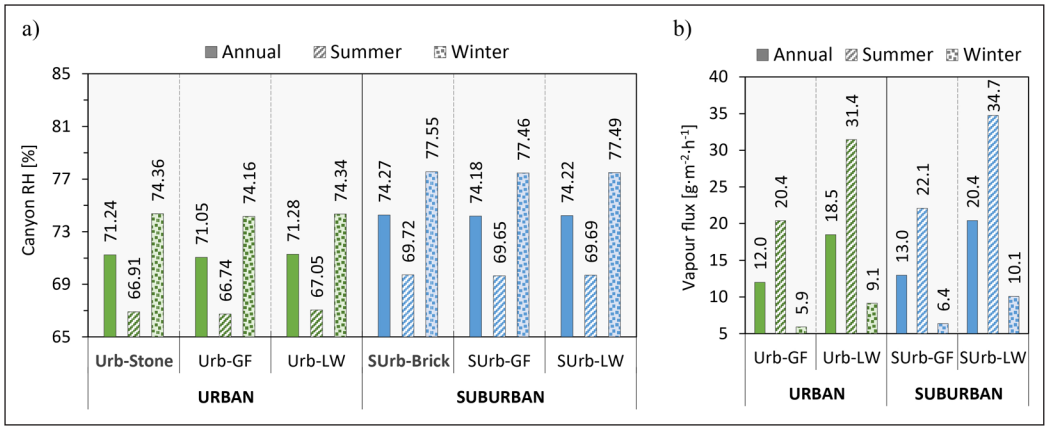

Figure 5: (a) Mean annual, summer and winter canyon relative humidity (RH_{can}); and **(b)** mean annual, summer and winter vapour flux densities for the scenarios.

The simulated canyon relative humidity (RH_{can}) highlighted higher mean values for the suburban scenarios than the urban (expected contribution from greater suburban green cover), while winter means were much greater than the summer for all scenarios (affected by background air temperature). The addition of VG to both urban and suburban scenarios marginally reduced means with GF application, while the converse was true with LW application (Figure 5a). Examining vapour flux densities highlighted summer contributions from VG to be significantly higher than in winter, with LW application patently contributing higher values than GF (Figure 5b).

3.2 CANYON BUILDING SURFACE TEMPERATURES AND SURFACE FLUX

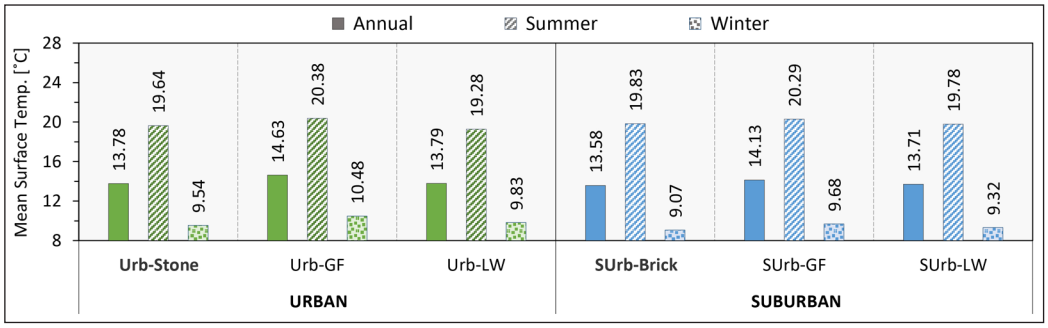

Figure 6: Mean annual, summer and winter canyon building wall temperatures ($T_{canWall}$) for the scenarios.

When summertime canyon building wall temperature ($T_{canWall}$) hourly means were considered, LW surfaces were marginally cooler than the respective base bare wall scenarios, while GF surfaces in contrast were warmer (Figure 6). Notably, LW canyon building wall temperature means were also cooler than GF means, with greater influence during the summer (1.10 and 0.51 K cooler relative to *Urb-GF* and *SUrb-GF* scenarios, respectively), than in winter (0.65 and 0.36 K cooler relative to *Urb-GF and SUrb-GF* scenarios, respectively).

The profiles for the summer solstice demonstrated higher canyon building wall temperatures ($T_{canWall}$) for *SUrb-Brick* surfaces relative to *Urb-Stone* (Figure 7a), while the converse was true with the winter solstice profiles (Figure 7b). VG addition reduced the peak to peak amplitudes to 'flatten/dampen' the $T_{canWall}$ profiles, which translated to cooler peak temperatures for the summer solstice and mostly (except for *SUrb-LW*) warmer peak temperatures for the winter solstice. The summer solstice cooling influence was greater with LW than GF profiles, while the winter solstice warming influence was greater with GF than LW profiles, with pronounced influence evident with urban scenarios. The solstice profiles for *Urb-Stone* and *SUrb-Brick* also indicated a temporal shift for when peak temperatures occur, with a lag of two hours for the summer and one for the winter solstice profiles. Adding VG marginally delayed the peak occurrence, with LW scenarios presenting a greater delay relative to GF scenarios.

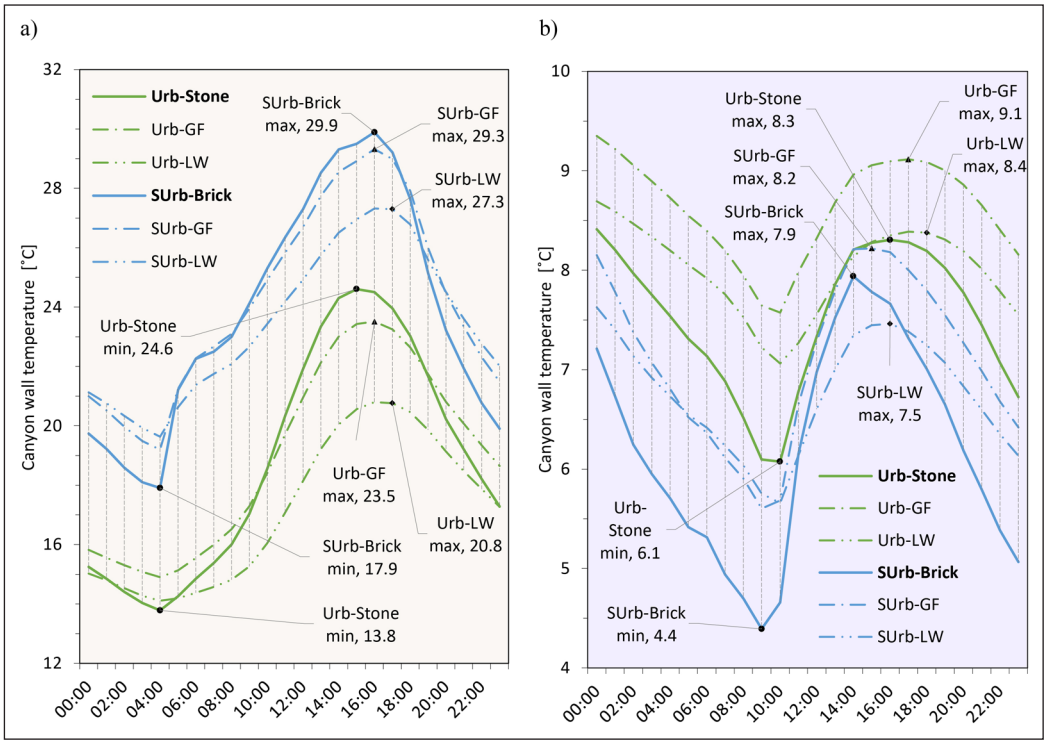

Figure 7: (a) Summer and **(b)** winter solstice building $T_{canWall}$ profiles for the scenarios.

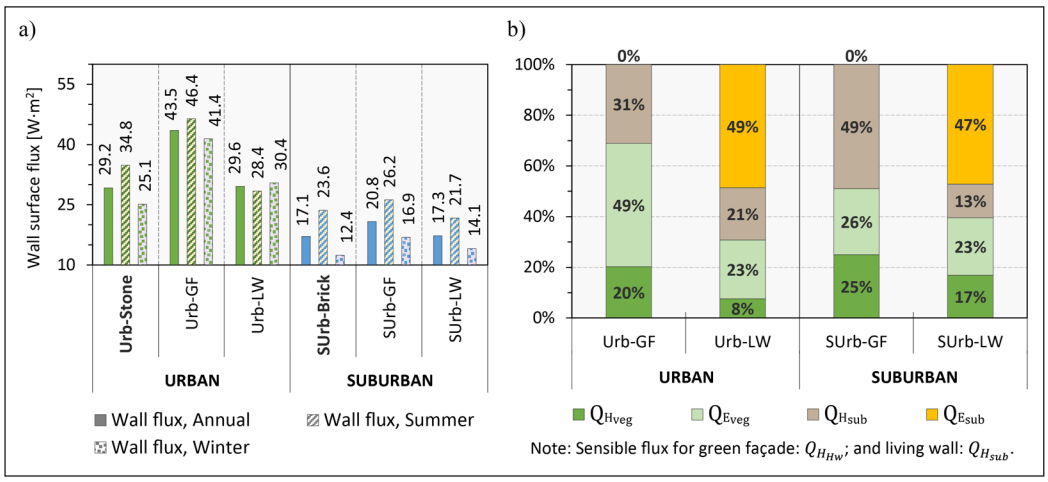

Figure 8: (a) Mean canyon $Q_{canWall}$ for the scenarios; and **(b)** mean canyon wall surface convective flux partitioning for the vertical greening scenarios.

Canyon wall surface flux ($Q_{canWall}$) data revealed urban mean values to be significantly higher than suburban, with summertime flux making dominant contributions in all except the urban LW application scenario (*i.e. Urb-LW*) (Figure 8a). GF applications made higher contribution relative to LW application scenarios, which was pronounced greatest for the urban context. The surface convective flux partitioning revealed LW substrate latent flux ($Q_{E_{sub}}$) to be dominant for both urban and suburban contexts, while GF host-wall sensible flux ($Q_{H_{Hw}}$) was dominant for the suburban, and vegetation sensible flux ($Q_{H_{veg}}$) was dominant for the urban context (Figure 8b).

3.3 CANYON BUILDING SPACE-CONDITIONING

Annual mean space-conditioning consumption was significantly higher for the suburban scenarios, with winter heating dominating. VG application had most impact on reducing mean summer heating consumption (transitional), followed by winter heating, winter cooling (transitional), and summer cooling. All means, therefore, were reduced to some extent, with reductions pronounced for the urban context than suburban, and with LW application than GF (Figure 9a).

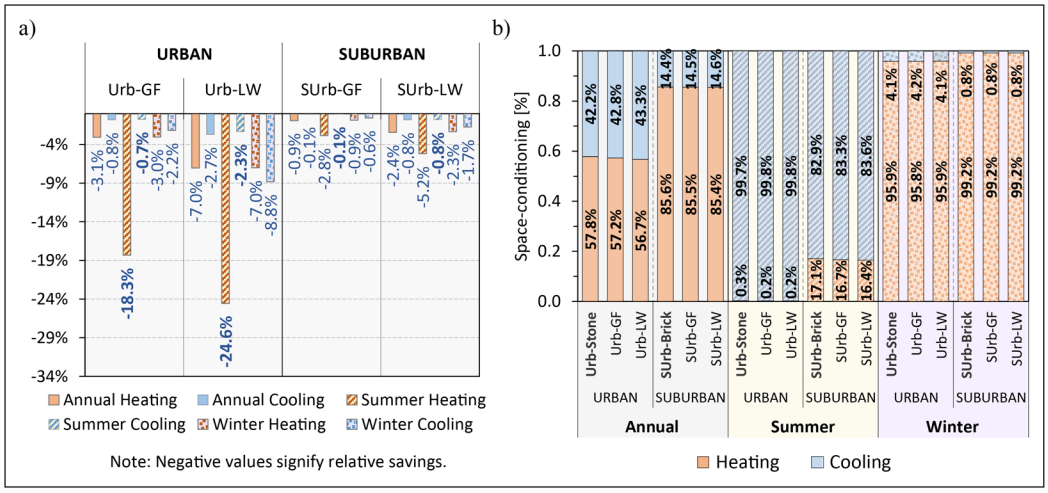

Figure 9: (a) Impact of vertical greening application on space-conditioning energy consumption relative to base wall scenarios; and **(b)** annual, summer and winter space-conditioning load partitioning for the scenarios.

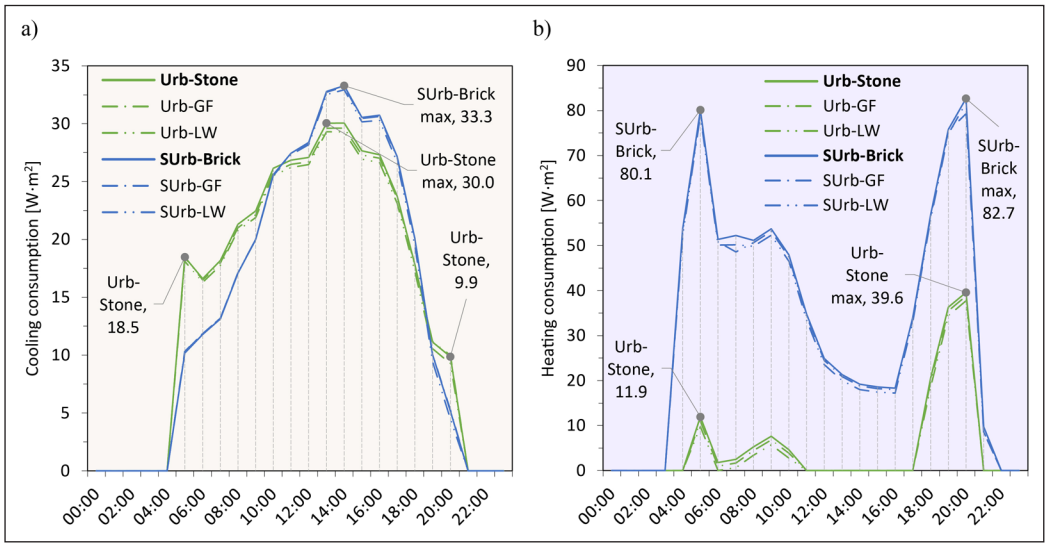

Figure 10: (a) Summer solstice cooling; and **(b)** winter solstice heating energy consumption profiles for the scenarios (per m^2 of building floor area).

Examining the summer solstice cooling consumption profiles highlighted urban scenarios to have a higher consumption period early in the morning (*i.e.* priming), and a relatively smaller, and shorter, higher consumption period later in the evening relative to suburban scenarios (Figure 10a). The suburban cooling peaks, however, were higher than the urban peaks. The winter solstice heating profiles in comparison showed significantly increased consumption for the suburban scenarios than urban, while both demonstrated twin peaks with one in the morning and the other later in the evening (Figure 10b). The solstice profiles in general demonstrated VG application to reduce consumption, mostly evident nearer to the peaks (Figure 10).

The space-conditioning energy consumption partitioning demonstrated cooling to be of greater significance to urban annual profiles than suburban (Figure 9b). In the summer, cooling consumption was near 100% for urban scenarios, while some transitional heating consumption was still evident for suburban scenarios (< 17.1%). This contrasted against the winter, where urban scenarios still presented some transitional cooling consumption (< 4.2%), while in the suburban context this was near negligible (< 0.8%).

4. DISCUSSION

The following discusses UWG plus VGM simulation outcomes including heat island influence and VG applications. Thereafter, it considers the significance of facade materials and their interaction with VG applications, followed by the impact of such applications on the indoor space-conditioning energy use of urban and suburban canyon buildings.

4.1 VERTICAL GREENING IN LONDON STREET CANYONS

Considering the aforementioned historic observations and trends for London, the heat island simulated by the UWG plus VGM coupling could be said to fall within a plausible range, with the urban base *Urb-Stone* scenario summertime daily mean intensity (ΔT_{UHI}) at 1.86, ±0.84 K (N = 153 days), and wintertime mean at 1.56, ±0.50 K (N = 212 days); while the suburban base *SUrb-Brick* scenario summertime daily mean intensity was 1.21, ±0.69 K, and wintertime mean at 0.94, ±0.33 K. The suburban scenario generated relatively milder canyon temperatures and as a result ΔT_{UHI}, which is illustrated by the summer solstice profiles (Figure 4). This urban to suburban disparity is consistent with observations noted earlier in relation to the decreasing heat island intensity trend when traversing away from the city centre and into the peripheries (Watkins *et al.* 2002); which is typically an indication of morphological spread (low density development), and associated changes in construction types, materiality and green cover.

The urban context simulations including canyon VG highlighted LW application to present a cooler summertime mean intensity at 1.81, ±0.83 K (N = 153 days), while its wintertime mean was barely changed. GF application in contrast presented the warmest summertime mean intensity at 1.89, ±0.85 K, as well as the warmest wintertime mean at 1.60, ±0.51 K (N = 212 days). In the suburban context, LW application contributed to a marginally cooler summertime mean, while the winter mean was warmer at 0.95, ±0.35 K. GF application again presented the warmest summertime mean at 1.23, ±0.69 K, as well as the warmest wintertime mean at 0.96, ±0.34 K. In summary, GF application in both contexts served to generate a warmer canyon heat island intensity to be experienced, while a cooler mean was only presented by the summer with LW application, and with much greater influence in the urban canyon than suburban.

The lower summertime heat island intensity means simulated for the day relative to the night-time is consistent with previous observations (Oke 1987). Howard's (1833) finding of a much cooler daytime mean temperature relative to the surroundings (*i.e.* cool island), however, was not relatable to any of the simulations. This is explained by the fact that cool island conditions simulated tended to be modest and restricted to shorter durations. This could be attributed to the north to south orientation and the 20 m width of the canyons minimising albedo and self-shading influence (key contributing factors) (Oke 1988). The urban versus suburban disparity could be attributed to the notably higher anthropogenic heat contribution used for the urban Moorgate context, in contrast to the suburban Wimbledon context (based on Iamarino *et al.* 2012), while the latter also included a higher proportion of the ground surface flux being partitioned as latent flux from its increased background vegetation cover.

Building fabrics with dominant heavyweight constructions are typically identified to generate a warmer heat island effect to be experienced in street canyons at night, while the converse may be true during the daytime (Gartland 2008; Gunawardena *et al.* 2019; Oke 1987). The denser stone material of the *Urb-Stone* base scenario generated greater night-time heat island hourly maxima occurrences in agreement, while in contrast the *SUrb-Brick* base scenario presented greater daytime cool island hourly occurrences. VG application modified these hourly maxima occurrences, with LW application in the urban context reducing night-time instances by 1.6% in the summer and 2.8% annually. This would offer some thermal relief, given that nocturnal temperatures are more oppressive to human health (Gunawardena 2015a, 2015b), although the canyon profile of including office use means that this modest benefit is unlikely to be experienced by pedestrians. Daytime cool island occurrences in contrast were increased with VG applications, with the urban canyon benefiting substantially with LW application to present a 38.8% increase in occurrences during the critical summer period (*i.e.* when heat relief is most sought), compared with a modest 3.4% increase for the suburban context. This could present significant value to daytime pedestrian comfort and thermal diversity (alliesthesia) associated enhancement in wellbeing (Parkinson & De Dear 2015). LW application in this regard offered greater summertime advantage in improving the urban canyon's thermal climate than suburban, while GF application benefit in both contexts was lower (12% and 3%, respectively).

These thermal influences, however, must also be considered in relation to humidity generation associated with installations. The increased vapor flux in the summer (Figure 5b) is explained by increased energy in the system facilitating greater evapotranspiration, while higher flux from LW application relative to GF is attributed mostly to the additional contribution from substrate moisture evaporation. The available research suggests the excess flux to be relevant only within a proximate zone fronting the installations, with background wind conditions in outdoor environments typically advecting away this excess to normalise to background levels (Blanc 2012; Gunawardena & Steemers 2021; Li *et al.* 2019). Any negative influences associated with humidity excess including thermal discomfort is therefore unlikely to be a significant burden to street canyon pedestrians.

4.2 VERTICAL GREENING INFLUENCE ON CANYON BUILDINGS

The materiality of the built environment affects net radiation and heat storage of the urban surface energy balance (Oke 1987). Material radiative properties are defined by emissivity and albedo, while heat storage is affected by mass, heat capacity and thermal conductivity. All these properties are intrinsic to the definition of any material, and as a result any construction assembly considered. Albedo has been established as a significant property (Gartland 2008), with higher values lowering radiation absorption by building facade materials to reduce their surface temperature, and as a result canyon wall temperature ($T_{canWall}$). The direct effect of this is to reduce canyon air temperature (T_{can}), as relatively cooler surfaces have lower sensible flux output to the canyon climate. The indirect effect works in conjunction with material emissivity and thermal storage properties to modify indoor building energy use and eventual anthropogenic heat emissions to the outdoor canyon climate.

This facade albedo influence benefited the untreated urban context considered in this study, where the stone was considered to be homogenous Portland (typical for Moorgate), which is of a lighter colouring and has a high mean albedo (about 0.6) (Yates 2017), relative to the outer-leaf brick considered for the suburban context (about 0.3). This difference in turn translated to temperature profile differences, as the stone reflected more energy into the urban canyon, relative to the brick in the suburban canyon. This explains the marginal reduction in the mean summertime canyon wall temperature for *Urb-Stone* relative to *SUrb-Brick* (Figure 6). The influence of albedo is also apparent in the canyon wall temperature summer solstice profiles, where the relatively lower albedo brick absorbed greater energy to present warmer wall temperatures than stone (Figure 7a). The higher absorption of the brick in turn translated to less energy being reflected back to the suburban canyon, which resulted in a lower peak ΔT_{UHI} than for the urban stone canyon, where the stone contributed more reflected energy as well as secondary reflections to encourage a higher canyon ΔT_{UHI} to be experienced (Figure 4b). It is also significant to note that the amplitude differences between these urban and suburban profiles are also affected by contributions from heat storage and morphological properties of the wider contexts (Oke 1987).

The delayed wall temperature peak (*i.e.* phase shift) of brick (Figure 7a) is explained by its thermal storage properties (Table 2), in particular, the relatively lower thermal conductivity and diffusivity of brick compared with stone. The brick as a result took longer to reach its peak capacity, relative to stone. The canyon air temperature lag for the summer solstice urban stone profile in contrast is explained by the secondary reflections delaying the canyon air mass reaching its capacity (Figure 4b). Wintertime interactions, however, are more complex to describe, given that there is greater thermal input from building interiors, coupled with the greater heat capacity of the stone construction relative to brick.

VG application to both urban and suburban scenarios served to add to the existing wall temperature phase shifts (Figure 7a). LW application notably presented a greater delay relative to GF, explained by the additional heat storage contributed by its 100 mm substrate zone. The influence of VG application is also demonstrated by the canyon wall temperature solstice profile peak to peak amplitudes (Figure 7a), where they were reduced to flatten or moderate fluctuations. The magnitude of these reductions was pronounced for peaks than troughs, with the peak damping presenting a beneficial summertime cooling influence, while the trough damping presented a wintertime warming benefit. This translated best with LW applications for longer durations,

where summer means were cooler (by 0.36 K relative to *Urb-Stone*; and by 0.05 K relative to *SUrb-Brick*), and winter means were warmer than base scenarios (by 0.29 K relative to *Urb-Stone*; and by 0.25 K relative to *SUrb-Brick*). This moderating benefit of LW application is explained by the joint action of added heat storage and the evaporative flux from the substrate and vegetation. The latter evaporative flux represented > 70% of the canyon wall convective surface flux, with marginally greater contribution in the urban context (72%). GF application, in contrast, presented warmer means for both summer (by 0.74 K relative to *Urb-Stone*; and by 0.46 K relative to *SUrb-Brick*), and winter periods (0.94 K relative to *Urb-Stone*; and by 0.61 K relative to *SUrb-Brick*). The insulating effect of the GF vegetation layer seemed to counter the cooling benefit offered from its evaporative flux, with the latter having represented a relatively moderate significance of 49% of the convective surface flux for the urban context, while in the suburban context represented a much lower contribution of 26% (Figure 8b).

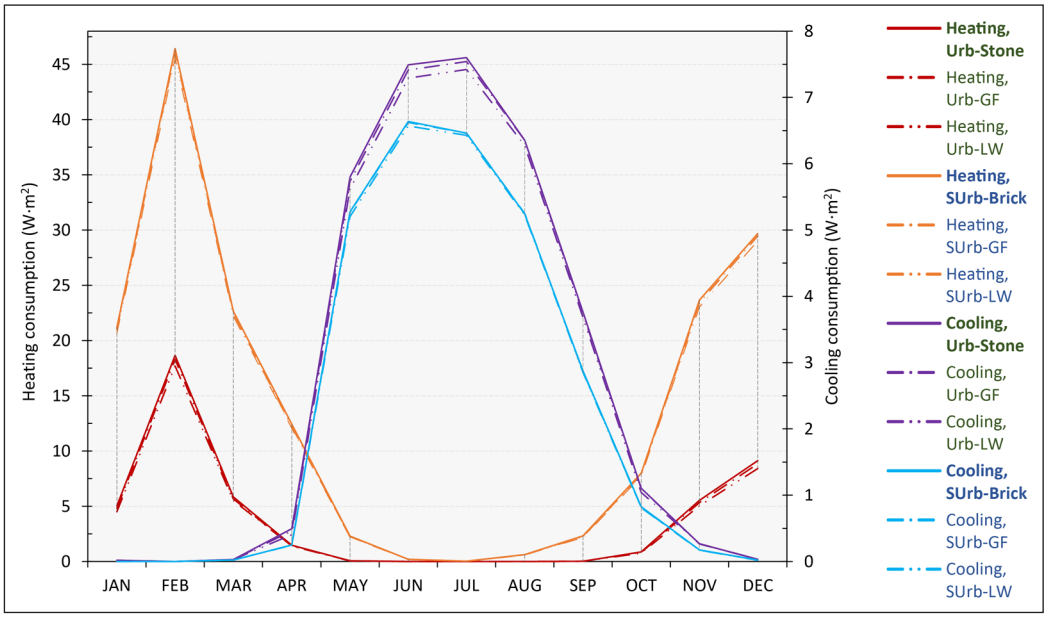

Figure 11: Monthly mean space-conditioning energy consumption *for the scenarios*.

The damping of summer and winter canyon wall temperature peaks following VG application translated to reductions in indoor space-conditioning energy consumption. All consumption demands were reduced to some extent, with reductions pronounced for the urban context than suburban, and as with the above canyon wall temperatures, translating to better performance from LW application than GF. Notably, the damping influence contributed to reducing relative summer heating consumption the most (in contrast to cooling consumption anticipated), while winter cooling load reductions were also pronounced. These loads were minimal by default (Figure 9b), and evident at summer to winter transitional periods. The damping influence of VG installations presented significant reductions for these loads, which although translated to considerable relative percentage reductions (Figure 9a), from a building space-conditioning profile perspective was less significant.

From a relative reduction perspective, summertime cooling consumption benefited the least from VG applications, while the winter heating consumption benefit was higher (Figure 9a). Although VG is commonly promoted as a summertime cooling contributor, the result of this study highlighted greater contribution as a thermal moderator that regulates fluctuations to also present significant benefit during the heating season (Figure 11). The relatively fewer studies that have considered the wintertime influence of building facade applications have observed this moderating effect with colder temperatures to offer thermal benefit (Libessart & Kenai 2018). Observational studies had identified the insulating and shielding thermal benefits offered to reduce heating loads, while better performance was highlighted with increased cover and during relatively harsher background conditions (Bolton *et al.* 2014; Cameron *et al.* 2015). In agreement with the simulation results, a comparative study had also identified better performance with LW application relative to GF (Coma *et al.* 2017). Some LW, however, have reported negligible savings (Coma *et al.* 2020), and

a minority have even reported increased expenditure (Djedjig *et al.* 2017), which has suggested dependency on the description of the installations, particularly the substrate. The few studies that have considered the annual impacts of facade applications counter this potential shortcoming by stressing the requirement to assess net annual energy use. These identify such applications to still offer savings, if cooling energy expenditure is relevant for the building profile (Djedjig *et al.* 2017). In agreement, the net annual influence of VG applications in this study presented savings, with urban scenarios presenting greater savings than suburban, and LW application presenting greater savings than GF (savings from *Urb-GF*: 2.1%; *Urb-LW*: 5.2%; *SUrb-GF*: 0.8%; and *SUrb-LW*: 2.2%). These, however, were modest than expected, and thus unlikely to justify deployment as an exclusive solution to conserve energy use. The net annual energy-use savings nevertheless highlight noteworthy contribution and potential to be incorporated into wider green infrastructure enhancement strategies in temperate climate street canyons.

When used in conjunction with material heat storage in the right building locations and adequate night-time purge ventilation, VG applied heavyweight constructions could facilitate the creation of thermally comfortable indoor environments with reduced space-conditioning loads in both summer and winter. This presents an alternative approach to enhancing the performance of historic buildings that are often built with such constructions, and when other thermal retrofitting solutions might not be deemed appropriate. The net savings achieved, however, are dependent not only on the duration and magnitude of climate loading experienced, envelope constructions and their thermal resistances, but also on the relevant occupancy groups and their activity schedules. Furthermore, net annual benefits can only be realised with the successful growth of evergreen flora, which means that greater attention needs to be given to identifying flora with sufficient 'hardiness ratings' to sustain ecosystem service provision throughout the challenging winter months.

5. CONCLUSIONS

This paper considered the extent to which neighbourhood-scale application of vertical greening (VG) contributes to enhancing urban climate resilience. It examined this through a simulation comparison study of office building construction build-ups including VG applications—both green facade (GF) and living wall (LW)—sited within the morphological contexts of central urban and suburban neighbourhoods (*i.e.* within London's heat island core and towards its periphery). The study simulated the respective street canyon scenarios using a pathway coupling an established multiscale urban climate framework and a novel vertical greening model (VGM).

Table 4: Summary of the influence of vertical greening application on space-conditioning energy consumption.

Note: Negative values signify savings relative to the base bare stone/brick scenarios.

	ANNUAL (%)				SUMMER (%)				WINTER (%)			
	URB-STONE		*SURB-BRICK*		*URB-STONE*		*SURB-BRICK*		*URB-STONE*		*SURB-BRICK*	
	GF	LW	GF	LW	GF	LW	GF	LW	GF	LW	GF	LW
Relative to base	−2.1%	−5.2%	−0.8%	−2.2%	−0.8%	−2.4%	−0.5%	−1.5%	−3.0%	−7.1%	−0.9%	−2.3%
Heating	−3.1%	−7.0%	−0.9%	−2.4%	−18.3%	−24.6%	−2.8%	−5.2%	−3.0%	−7.0%	−0.9%	−2.3%
Cooling	−0.8%	−2.7%	−0.1%	−0.8%	−0.7%	−2.3%	−0.1%	−0.8%	−2.2%	−8.8%	−0.6%	−1.7%
Relative to GF		−3.2%		−1.4%		−1.6%		−1.0%		−4.2%		−1.5%
Heating		−4.1%		−1.5%		−7.6%		−2.4%		−4.1%		−1.5%
Cooling		−1.9%		−0.7%		−1.6%		−0.7%		−6.8%		−1.2%

The simulation results demonstrated the application of VG to present immediate benefit to canyon pedestrians in the form of reduced daytime heat island intensity, as well as increased occurrences of cool island conditions experienced (summer daytime occurrences increased by 39% for central urban and 3.4% for suburban canyons). These effects were pronounced for the urban setting than suburban, while LW application offered greater advantage towards improving the urban canyon climate.

These canyon thermal climate improvements also translated to net annual space-conditioning savings for the buildings fronting the canyons (between 0.8% and 5.2%) (see the summary in Table 4), with urban scenarios presenting greater savings than suburban, and the LW application presenting greater savings than GF. In summary, these results suggest LW application in dense urban canyon configurations to present the best thermal and associated energy-use outcomes, which should in turn inform the future specification and siting of such installations. While net annual savings of such arrangements may present potential for wider implementation in temperate climates, the magnitudes of thermal and energy-use benefits gained are unlikely to justify their use as an exclusive solution. Such installations are therefore best regarded as belonging to a suite of solutions that can be implemented to mitigate heat-related risks and conserve energy in densely constructed urban environments. Furthermore, any widescale application proposals would also require assessment against other ecosystem service provisions, as well as costs associated with maintaining flourishing installations.

ACKNOWLEDGEMENTS

The authors thank the Engineering and Physical Sciences Research Council of the United Kingdom.

AUTHOR AFFILIATIONS

Kanchane Gunawardena orcid.org/0000-0002-6278-3755
The Martin Centre for Architectural and Urban Studies, Department of Architecture, University of Cambridge, Cambridge, UK

Koen Steemers orcid.org/0000-0001-8135-158X
The Martin Centre for Architectural and Urban Studies, Department of Architecture, University of Cambridge, Cambridge, UK

AUTHOR CONTRIBUTIONS

K.G.: Principal author; research design; data acquisition, analysis and interpretation; K.S: Project principal investigator, supervisor, concept design advisor and draft reviewer.

COMPETING INTERESTS

The authors have no competing interests to declare.

FUNDING

This study was funded by UK Research & Innovation (UKRI) (grant number 1930753).

REFERENCES

Alexandri, E., & **Jones, P.** (2007). Developing a one-dimensional heat and mass transfer algorithm for describing the effect of green roofs on the built environment: Comparison with experimental results. *Building and Environment*, 42(8), 2835–2849. DOI: https://doi.org/10.1016/j.buildenv.2006.07.004

Allen, R. G., Pereira, L. S., Raes, D., & **Smith, M.** (1998). *Crop evapotranspiration—Guidelines for computing crop water requirements* (FAO Irrigation and Drainage Paper No. 56, 300(9), D05109). Food and Agriculture Organization (FAO).

Blanc, P. (2012). *The vertical garden: From nature to the city*, revd edn, ed. V. Lalot. W. W. Norton.

Bolton, C., Rahman, M. A., Armson, D., & **Ennos, A. R.** (2014). Effectiveness of an ivy covering at insulating a building against the cold in Manchester, UK: A preliminary investigation. *Building and Environment*, 80, 32–35. DOI: https://doi.org/10.1016/j.buildenv.2014.05.020

Bueno, B., Norford, L., Hidalgo, J., & **Pigeon, G.** (2013). The urban weather generator. *Journal of Building Performance Simulation*, 6(4), 269–281. DOI: https://doi.org/10.1080/19401493.2012.718797

Bueno, B., Roth, M., Norford, L., & **Li, R.** (2014). Computationally efficient prediction of canopy level urban air temperature at the neighbourhood scale. *Urban Climate*, 9, 35–53. DOI: https://doi.org/10.1016/j.uclim.2014.05.005

Bueno, B., Sullivan, J., Street, M., … Gunawardena, K. (2019). *Urban Weather Generator (V5.1.0 beta)*. University of Cambridge.

Bueno, B., Sullivan, J., Street, M., Zhang, L., & **Lopez-Pineda, B. T.** (2015). *Urban Weather Generator (V4.1.0)*. Building Technology Program, Massachusetts Institute of Technology.

Cameron, R. W. F., Taylor, J., & **Emmett, M.** (2015). A Hedera green façade—Energy performance and saving under different maritime-temperate, winter weather conditions. *Building and Environment*, 92, 111–121. DOI: https://doi.org/10.1016/j.buildenv.2015.04.011

Chandler, T. J. (1965). *The climate of London*. Hutchinson.

Coma, J., Chàfer, M., Pérez, G., & **Cabeza, L. F.** (2020). How internal heat loads of buildings affect the effectiveness of vertical greenery systems? An experimental study. *Renewable Energy*, 151, 919–930. DOI: https://doi.org/10.1016/j.renene.2019.11.077

Coma, J., Pérez, G., de Gracia, A., Burés, S., Urrestarazu, M., & **Cabeza, L. F.** (2017). Vertical greenery systems for energy savings in buildings: A comparative study between green walls and green facades. *Building and Environment*, 111, 228–237. DOI: https://doi.org/10.1016/j.buildenv.2016.11.014

Davis, M. M., Vallejo Espinosa, A. L., & **Ramirez, F. R.** (2019). Beyond green façades: Active air-cooling vertical gardens. *Smart and Sustainable Built Environment*, 8(3), 243–252. DOI: https://doi.org/10.1108/SASBE-05-2018-0026

de Jesus, M. P., Lourenço, J. M., Arce, R. M., & **Macias, M.** (2017). Green façades and in situ measurements of outdoor building thermal behaviour. *Building and Environment*, 119, 11–19. DOI: https://doi.org/10.1016/j.buildenv.2017.03.041

Di, H. F., & **Wang, D.** (1999). Cooling effect of ivy on a wall. *Experimental Heat Transfer*, 12(3), 235–245. DOI: https://doi.org/10.1080/089161599269708

Djedjig, R., Belarbi, R., & **Bozonnet, E.** (2017). Experimental study of green walls impacts on buildings in summer and winter under an oceanic climate. *Energy and Buildings*, 150, 403–411. DOI: https://doi.org/10.1016/j.enbuild.2017.06.032

Djedjig, R., Bozonnet, E., & **Belarbi, R.** (2016). Modeling green wall interactions with street canyons for building energy simulation in urban context. *Urban Climate*, 16, 75–85. DOI: https://doi.org/10.1016/j.uclim.2015.12.003

Djedjig, R., Ouldboukhitine, S. E., Belarbi, R., & **Bozonnet, E.** (2012). Development and validation of a coupled heat and mass transfer model for green roofs. *International Communications in Heat and Mass Transfer*, 39(6), 752–761. DOI: https://doi.org/10.1016/j.icheatmasstransfer.2012.03.024

Doick, K. J., Peace, A., & **Hutchings, T. R.** (2014). The role of one large greenspace in mitigating London's nocturnal urban heat island. *Science of the Total Environment*, 493, 662–671. DOI: https://doi.org/10.1016/j.scitotenv.2014.06.048

Eames, M., Kershaw, T., & **Coley, D.** (2011). On the creation of future probabilistic design weather years from UKCP09. *Building Services Engineering Research & Technology*, 32(2), 127–142. DOI: https://doi.org/10.1177/0143624410379934

Gartland, L. (2008). *Heat islands: Understanding and mitigating heat in urban areas*. Earthscan/Routledge.

Giridharan, R., & **Kolokotroni, M.** (2009). Urban heat island characteristics in London during winter. *Solar Energy*, 83(9), 1668–1682. DOI: https://doi.org/10.1016/j.solener.2009.06.007

Grimmond, C. S. B., Blackett, M., Best, M. J., … Zhang, N. (2010). The International Urban Energy Balance Models Comparison Project: First results from Phase 1. *Journal of Applied Meteorology and Climatology*, 49(6), 1268–1292. DOI: https://doi.org/10.1175/2010JAMC2354.1

Gunawardena, K. R. (2015a). Heat vulnerability: Risk to health and wellbeing in the built environment (MPhil paper, University of Cambridge).

Gunawardena, K. R. (2015b). Residential overheating risk in an urban climate (MPhil dissertation, University of Cambridge).

Gunawardena, K. (2018a). Fundamentals of urban heat islands: Concise guide for architects and urban planners (PhD paper, University of Cambridge).

Gunawardena, K. (2018b). Methodologies for assessing urban microclimates (PhD paper, University of Cambridge). DOI: https://doi.org/10.13140/RG.2.2.11610.41921

Gunawardena, K., Kershaw, T., & **Steemers, K.** (2019). Simulation pathway for estimating heat island influence on urban/suburban building space-conditioning loads and response to facade material changes. *Building and Environment*, 150(January), 195–205. DOI: https://doi.org/10.1016/j.buildenv.2019.01.006

Gunawardena, K., & **Steemers, K.** (2019a). Adaptive comfort assessments in urban neighbourhoods: Simulations of a residential case study from London. *Energy and Buildings*, 202, 109322. DOI: https://doi.org/10.1016/j.enbuild.2019.07.039

Gunawardena, K., & **Steemers, K.** (2019b). Living walls in indoor environments. *Building and Environment*, 148, 478–487. DOI: https://doi.org/10.1016/j.buildenv.2018.11.014

Gunawardena, K., & **Steemers, K.** (2020). Characterising living wall microclimate modifications in sheltered urban conditions: Findings from two monitored case studies. In J. Rodríguez-Álvarez & J. C. Gonçalves (Eds.), *Planning post carbon cities. Proceedings of the 35th PLEA Conference on Passive and Low Energy Architecture*. Volume 1 (pp. 606–611). University of A Coruña. DOI: https://doi.org/10.17863/CAM.58491

Gunawardena, K., & **Steemers, K.** (2021). Living wall influence on the microclimates of sheltered urban conditions: Results from monitoring studies. *Architectural Science Review*, 64(3), 235–246. DOI: https://doi.org/10.1080/00038628.2020.1812501

Gunawardena, K., & **Steemers, K.** (2022). Including indoor vertical greening installation influence in building thermal and energy use simulations. In W. Bustamante, M. Andrade, & P. Ortiz E. (Eds.), *Will cities survive?: Proceedings of the 36th PLEA Conference on Passive and Low Energy Architecture* (pp. 124–28). Pontifical Catholic University of Chile. DOI: https://doi.org/10.17863/CAM.91868

Gunawardena, K. R. (2021). Vertical greening in urban built environments (PhD dissertation, University of Cambridge). DOI: https://doi.org/10.17863/CAM.82336

Gunawardena, K. R., & **Kershaw, T.** (2016). Green and Blue-Space Significance to Urban Heat Island Mitigation—University of Bath's research portal. In S. Emmit & K. Adeyeye (Eds.), *Integrated Design International Conference (ID@50)* (pp. 1–15). University of Bath.

Gunawardena, K. R., & **Kershaw, T.** (2017). Urban climate influence on building energy use. In M. Burlando, M. Canepa, A. Magliocco, K. Perini, & M. P. Repetto (Eds.), *International Conference on Urban Comfort and Environmental Quality URBAN-CEQ* (pp. 175–184). Genoa University Press. http://digital.casalini.it/9788897752912

Gunawardena, K. R., Wells, M. J., & **Kershaw, T.** (2017c). Utilising green and bluespace to mitigate urban heat island intensity. *Science of the Total Environment*, 584–585, 1040–1055. DOI: https://doi.org/10.1016/j.scitotenv.2017.01.158

Holm, D. (1989). Thermal improvement by means of leaf cover on external walls—A simulation model. *Energy and Buildings*, 14(1), 19–30. DOI: https://doi.org/10.1016/0378-7788(89)90025-X

Howard, L. (1833). *The climate of London, deduced from meteorological observations, made in the metropolis, and at various places around it*, 3 vols. Harvey & Darton, J. & A. Arch, Longman & Co., Hatchard & Son, S. Highley, and R. Hunter.

Iamarino, M., Beevers, S., & **Grimmond, C. S. B.** (2012). High-resolution (space, time) anthropogenic heat emissions: London 1970–2025. *International Journal of Climatology*, 32(11), 1754–1767. DOI: https://doi.org/10.1002/joc.2390

Jones, P. D., & **Lister, D. H.** (2009). The urban heat island in Central London and urban-related warming trends in Central London since 1900. *Weather*, 64(12), 323–327. DOI: https://doi.org/10.1002/wea.432

Kershaw, T., Sanderson, M., Coley, D., & **Eames, M.** (2010). Estimation of the urban heat island for UK climate change projections. *Building Services Engineering Research and Technology*, 31(3), 251–263. DOI: https://doi.org/10.1177/0143624410365033

Kolokotroni, M., & **Giridharan, R.** (2008). Urban heat island intensity in London: An investigation of the impact of physical characteristics on changes in outdoor air temperature during summer. *Solar Energy*, 82(11), 986–998. DOI: https://doi.org/10.1016/j.solener.2008.05.004

Kolokotroni, M., Zhang, Y., & **Giridharan, R.** (2009). Heating and cooling degree day prediction within the London urban heat island area. *Building Services Engineering Research and Technology*, 30(3), 183–202. DOI: https://doi.org/10.1177/0143624409104733

Kolokotroni, M., Zhang, Y. P., & **Watkins, R.** (2007). The London heat island and building cooling design. *Solar Energy*, 81(1), 102–110. DOI: https://doi.org/10.1016/j.solener.2006.06.005

Koyama, T., Yoshinaga, M., Hayashi, H., Maeda, K. Ichiro, & **Yamauchi, A.** (2013). Identification of key plant traits contributing to the cooling effects of green façades using freestanding walls. *Building and Environment*, 66, 96–103. DOI: https://doi.org/10.1016/j.buildenv.2013.04.020

Lee, D. O. (1992). Urban warming?—An analysis of recent trends in London's urban heat island. *Weather*, 47(2), 50–56. DOI: https://doi.org/10.1002/j.1477-8696.1992.tb05773.x

Li, C., Wei, J., & **Li, C.** (2019). Influence of foliage thickness on thermal performance of green façades in hot and humid climate. *Energy and Buildings*, 199, 72–87. DOI: https://doi.org/10.1016/j.enbuild.2019.06.045

Libessart, L., & **Kenai, M. A.** (2018). Measuring thermal conductivity of green-walls components in controlled conditions. *Journal of Building Engineering*, 19, 258–265. DOI: https://doi.org/10.1016/j.jobe.2018.05.016

Moffitt, B. J. (1972). The effects of urbanization on mean temperatures at Kew observatory. *Weather*, 27, 121–129. DOI: https://doi.org/10.1002/j.1477-8696.1972.tb04273.x

Monin, A. S., & **Obukhov, A. M.** (1988). Momentum and heat exchanges with homogeneous surfaces. In S. P. Arya (Ed.), *Introduction to micrometeorology*, 42, 157–181. Academic Press. DOI: https://doi.org/10.1016/S0074-6142(08)60426-X

Nakano, A., Bueno, B., Norford, L., & **Reinhart, C. F.** (2015). Urban Weather Generator—A novel workflow for integrating urban heat island effect within urban design process. *Building Simulation 2015*. International Building Performance Simulation Association. http://hdl.handle.net/1721.1/108779. DOI: https://doi.org/10.26868/25222708.2015.2909

Oke, T. R. (1987). *Boundary layer climates*, 2nd edn. Methuen.

Oke, T. R. (1988). Street design and urban canopy layer climate. *Energy and Buildings*, 11(1–3), 103–113. DOI: https://doi.org/10.1016/0378-7788(88)90026-6

Olivieri, F., Grifoni, R. C., Redondas, D., Sánchez-Reséndiz, J. A., & **Tascini, S.** (2017). An experimental method to quantitatively analyse the effect of thermal insulation thickness on the summer performance of a vertical green wall. *Energy and Buildings*, 150, 132–148. DOI: https://doi.org/10.1016/j.enbuild.2017.05.068

Parkinson, T., & **De Dear, R.** (2015). Thermal pleasure in built environments: Physiology of alliesthesia. *Building Research & Information*, 43(3), 288–301. DOI: https://doi.org/10.1080/09613218.2015.989662

Sailor, D. J. (2008). A green roof model for building energy simulation programs. *Energy and Buildings*, 40(8), 1466–1478. DOI: https://doi.org/10.1016/j.enbuild.2008.02.001

Susorova, I., Angulo, M., Bahrami, P., & **Stephens, B.** (2013). A model of vegetated exterior facades for evaluation of wall thermal performance. *Building and Environment*, 67, 1–13. DOI: https://doi.org/10.1016/j.buildenv.2013.04.027

Tudiwer, D., & **Korjenic, A.** (2017). The effect of living wall systems on the thermal resistance of the façade. *Energy and Buildings*, 135, 10–19. DOI: https://doi.org/10.1016/j.enbuild.2016.11.023

Watkins, R., Palmer, J., Kolokotroni, M., & **Littlefair, P.** (2002). The London heat island: Results from summertime monitoring. *Building Services Engineering Research and Technology*, 23(2), 97–106. DOI: https://doi.org/10.1191/0143624402bt031oa

Wilby, R. L. (2003). Past and projected trends in London's urban heat island. *Weather*, 58, 251–260. DOI: https://doi.org/10.1256/wea.183.02

Wong, N. H., Tan, A. Y. K., Chen, Y., … Wong, N. C. (2010). Thermal evaluation of vertical greenery systems for building walls. *Building and Environment*, 45(3), 663–672. DOI: https://doi.org/10.1016/j.buildenv.2009.08.005

Yates, T. (2017). *Jordans basebed technical data sheet*. Building Research Establishment (BRE) with Albion Stone.

TO CITE THIS ARTICLE:
Gunawardena, K., & Steemers, K. (2023). Assessing the influence of neighbourhood-scale vertical greening application. *Buildings and Cities*, 4(1), pp. 103–123. DOI: https://doi.org/10.5334/bc.282

Submitted: 21 December 2022
Accepted: 17 March 2023
Published: 24 April 2023

Buildings and Cities is a peer-reviewed open access journal published by Ubiquity Press.